

RESEARCH LETTER

Mutant KRAS Exosomes Alter the Metabolic State of Recipient Colonic Epithelial Cells



See editorial on page 647.

In colorectal cancer (CRC) cells, mutant Kirsten rat sarcoma (KRAS) cell-autonomously imparts Warburg-like¹ metabolic changes through induction of Glucose transporter 1 (GLUT-1) (SLC2A1).^{2,3} We previously reported that mutant KRAS has marked effects on the constituents of CRC exosomes,

including proteins and enzymes involved in metabolism and glycolysis.^{4,5} The present studies were designed to test whether mutant KRAS exosomes can alter the metabolic state cell-nonautonomously in recipient colonic epithelial cells.

We isolated exosomes purified from Daniel L. Dexter derived 1 (DLD-1) cells, which contain 1 wild-type (WT) and 1 mutant KRAS allele, and those from DLD-1 isogenic cell variants genetically engineered to express only the WT KRAS allele (DKs-8) or only the mutant KRAS allele (DKO-1).⁶ Adding DKO-1 exosomes to DKs-8 cells significantly reduced glucose concentrations in the medium, suggesting increased

cellular glucose uptake in these WT KRAS cells (Figure 1A). After 48-hour exposure to DKO-1 exosomes, a significantly higher percentage of recipient DKs-8 cells were in S and G2/M phases of the cell cycle (Supplementary Figure 1A and B), and cell number was increased at 120 hours (Supplementary Figure 1C). We next used the endogenous fluorescent characteristics of Nicotinamide adenine dinucleotide reduced (NADH) and Flavin adenine dinucleotide (FAD) to determine the relative balance between glycolysis and oxidative phosphorylation, as previously reported.⁷⁻⁹ Addition of mutant KRAS exosomes selectively and significantly increased

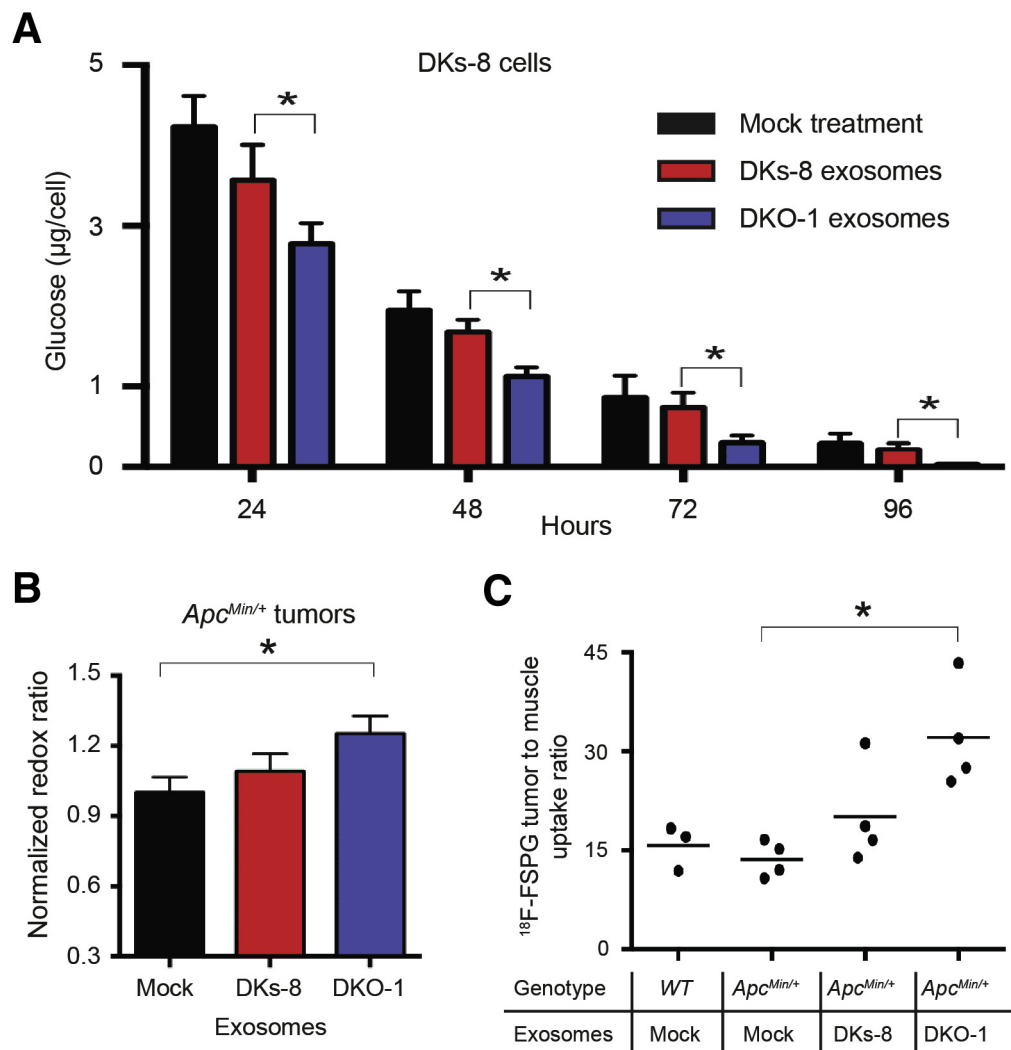


Figure 1. Mutant KRAS exosomes alter metabolism in vitro and in vivo. (A) Glucose consumption of exosome-treated DKs-8 cells (N = 3 in triplicate). Data are plotted as means ± SD. (B) Normalized redox ratio of exosome-treated *Apc^{Min/+}* colonic tumors. (C) ¹⁸F-FSPG tumor-to-muscle uptake ratio in WT or *Apc^{Min/+}* mice injected with exosomes analyzed by 1-way analysis of variance followed by a post hoc Tukey test. *P < .05.

the redox ratio in recipient normal mouse colonic cells cultured in Matrigel or on plastic (Supplementary Figure 2A–D) and WT KRAS DKs-8 cells (Supplementary Figure 2E).

To test whether mutant KRAS CRC exosomes function *in vivo*, we used the Adenomatous polyposis coli multiple intestinal neoplasia (*Apc^{Min/+}*) mouse model in which adenomas develop throughout the gastrointestinal tract. *Apc^{Min/+}* mice received intraperitoneal injections of DKs-8 or DKO-1 exosomes over 4 successive days. The redox ratio of tumors treated with DKO-1 exosomes was increased significantly (Figure 1B and Supplementary

Figure 3A), suggesting that treatment with these mutant KRAS exosomes increases aerobic glycolysis in recipient tumor cells. We also performed (S)-4-(3-[¹⁸F]-fluoropropyl)-L-glutamic acid (¹⁸F-FSPG) positron emission tomography imaging 2 hours after the last injection of exosomes. ¹⁸F-FSPG is a novel positron emission tomography tracer that follows the import of cystine by the glutamate/cystine antiporter *SLC7A11*, which is overexpressed in CRC.¹⁰ We found that *Apc^{Min/+}* mice injected with DKO-1 exosomes had a significant increase in ¹⁸F-FSPG uptake in the tumor region (Figure 1C and Supplementary Figure 3B and C),

suggesting that mutant KRAS CRC exosomes can alter tumor cell metabolism *in vivo*.

Levels of GLUT-1 were increased in DKO-1 exosomes, as well as in cell lysates (Figure 2A). To test whether these mutant KRAS exosomes contained functional GLUT-1, we measured ¹⁸F-fluorodeoxyglucose incorporation. After 1 hour, ¹⁸F-fluorodeoxyglucose uptake was significantly higher in DKO-1 exosomes (Figure 2B). The purified exosomes showed the characteristic cup-shaped morphology and size reported for exosomes (40–100 nm) (Supplementary Figure 4A and B). Further purification of exosomes on an

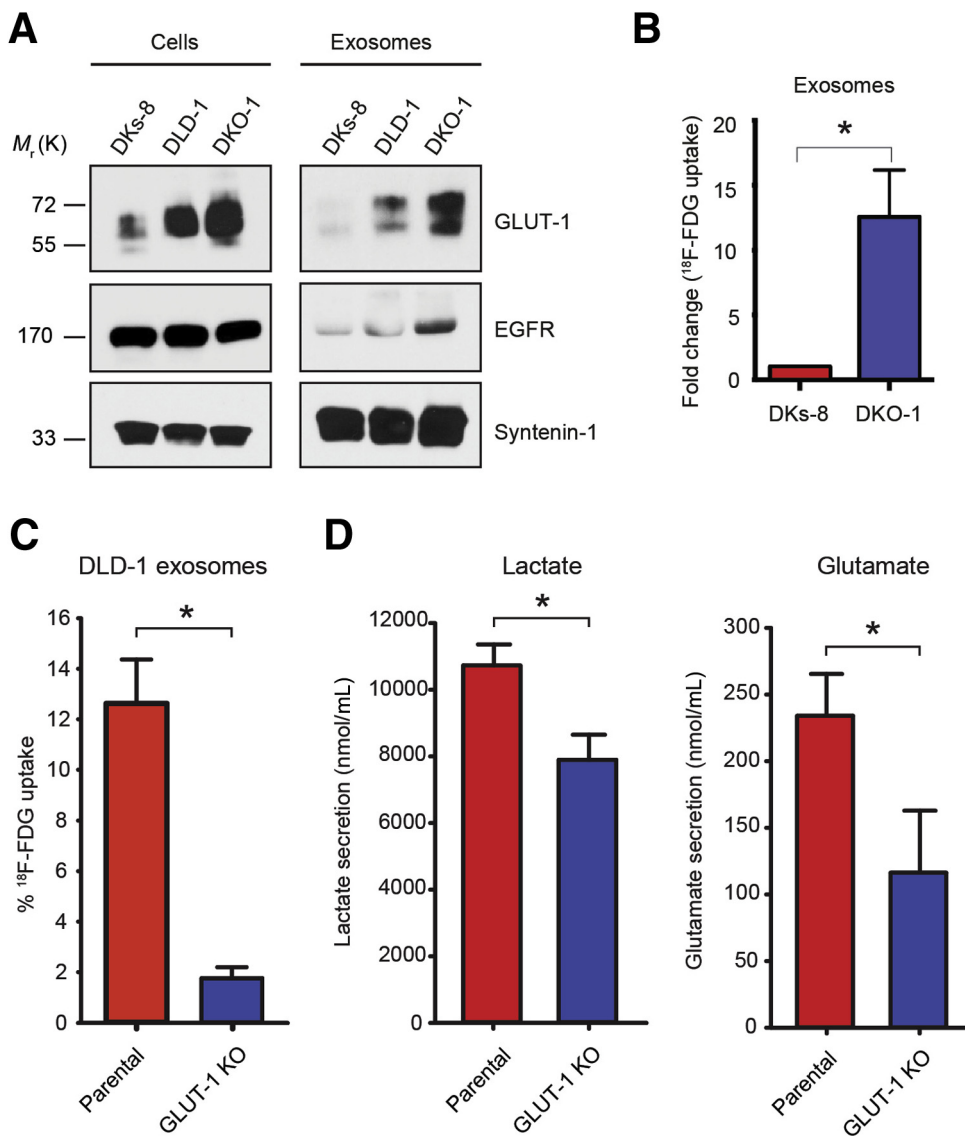


Figure 2. Exosomal GLUT-1 partially drives metabolic changes in recipient cells. (A) Immunoblot analysis of cells and exosomes. After normalization to syntenin-1, levels of GLUT-1 were increased 2.5- and 3.1-fold in cell lysates and 3.1- and 5.2-fold in exosomes of DLD-1 and DKO-1 cells, respectively. (B) Percent ¹⁸F-fluorodeoxyglucose (¹⁸FDG) uptake in exosomes isolated from DKs-8 and DKO-1 cells (N = 3 in triplicate). (C) Fold change of ¹⁸FDG uptake in exosomes isolated from parental and GLUT-1 KO DLD-1 cells. (D) nuclear magnetic resonance (NMR) determination of glutamate and lactate secretion in recipient DLD-1 GLUT-1 KO cells 43 hours after treatment with exosomes from parental DLD-1 or GLUT-1 KO cells (N = 2 in triplicate). Data are plotted as the means ± SD. *P < .05.

iodixanol density gradient showed that GLUT-1 was present in the fractions that contain established exosomal markers (Supplementary Figure 4C). Thus, mutant KRAS exosomes contain increased levels of functional GLUT-1.

Targeted disruptions of both alleles of *GLUT1* in DLD-1 cells (GLUT-1 knockout [KO]) led to loss of detectable GLUT-1 protein (Supplementary Figure 4D) and significantly reduced uptake of radiolabeled glucose in these exosomes (Figure 2C). None of the other glucose transporters tested (GLUT-2, GLUT-3, and GLUT-4) were detected in these exosomes (data not shown). We treated recipient DLD-1 GLUT-1 KO cells with exosomes isolated from DLD-1 parental or GLUT-1 KO cells for 43 hours and measured metabolite uptake and secretion using ¹H-MRS. Compared with GLUT-1 KO exosomes, parental DLD-1 exosomes significantly increased secretion of lactate and glutamate in recipient cells (Figure 2D), suggesting that exosomal GLUT-1 contributes to the altered metabolic state of recipient cells.

In summary, we show that mutant KRAS exosomes are able to confer a Warburg-like effect on recipient colonic epithelial cells in vitro and in vivo. Increased functional exosomal GLUT-1 contributes to metabolic changes in recipient cells. These preliminary observations should prompt further study of exosomes in tumor metabolism.

QIN ZHANG,^{1,*} DENNIS K. JEPPESEN,^{1,*}
JAMES N. HIGGINBOTHAM,^{1,*}
MICHELLE DEMORY BECKLER,^{1,2,*}
EMILY J. POULIN,³ ALEX J. WALSH,^{4,5}
MELISSA C. SKALA,^{4,5} ELIOT
T. MCKINLEY,¹
H. CHARLES MANNING,^{2,4,6} MATTHEW
R. HIGHT,^{6,7} MICHAEL L. SCHULTE,^{2,6}
KIMBERLY R. WATT,^{1,8}
G. DANIEL AYERS,⁹ MELISSA
M. WOLF,^{10,11}
GABRIELA ANDREJEVA,^{10,11} JEFFREY
C. RATHMELL,^{10,11,12} JEFFREY
L. FRANKLIN,^{1,3,8,13} ROBERT
J. COFFEY,^{1,3,13}

¹Department of Medicine, Vanderbilt University Medical Center, Nashville, Tennessee

²Department of Radiology, Vanderbilt University Medical Center, Nashville, Tennessee

³Department of Cell and Developmental Biology, Vanderbilt University Medical Center, Nashville, Tennessee

⁴Department of Biomedical Engineering, Vanderbilt University Medical Center, Nashville, Tennessee

⁵Morgridge Institute for Research, University of Wisconsin, Madison, Wisconsin

⁶Vanderbilt University Institute of Imaging Science, Vanderbilt University Medical Center, Nashville, Tennessee

⁷Department of Physics and Astronomy, Vanderbilt University Medical Center, Nashville, Tennessee

⁸Digestive Disease Research Center, Vanderbilt University Medical Center, Nashville, Tennessee

⁹Biostatistics Center, Vanderbilt University Medical Center, Nashville, Tennessee

¹⁰Department of Pathology, Microbiology, and Immunology, Vanderbilt University Medical Center, Nashville, Tennessee

¹¹Vanderbilt Center for Immunobiology, Vanderbilt University Medical Center, Nashville, Tennessee

¹²Department of Cancer Biology, Vanderbilt University, Nashville, Tennessee

¹³Department of Veterans Affairs Medical Center, Nashville, Tennessee
Corresponding author: e-mail: robert.coffey@vanderbilt.edu.

References

- Vander Heiden MG, et al. *Science* 2009;324:1029–1033.
- Iwamoto M, et al. *J Nucl Med* 2014; 55:2038–2044.
- Yun J, et al. *Science* 2009; 325:1555–1559.
- Demory Beckler M, et al. *Mol Cell Proteomics* 2013;12:343–355.
- Higginbotham JN, et al. *Curr Biol* 2011;21:779–786.
- Shirasawa S, et al. *Science* 1993; 260:85–88.
- Walsh A, et al. *Biomed Opt Express* 2012;3:75–85.


8. Walsh AJ, et al. *Cancer Res* 2013; 73:6164–6174.

9. Walsh AJ, et al. *J Biomed Opt* 2012;17:116015.

10. Jiang L, et al. *Nature* 2015; 520:57–62.

*Authors share coirst authorship.

Abbreviations used in this letter: Apc, adenomatous polyposis coli; CRC, colorectal cancer; DLD-1, Daniel L. Dexter derived 1; FAD, flavin adenine dinucleotide; ¹⁸F-FSPG, (S)-4-(3-[¹⁸F]-fluoropropyl)-L-glutamic acid; GLUT-1, glucose transporter 1; KO, knockout; KRAS, Kirsten rat sarcoma viral oncogene homolog; NADH, Nicotinamide adenine dinucleotide reduced; WT, wild-type

 Most current article

© 2018 The Authors. Published by Elsevier Inc. on behalf of the AGA Institute. This is an open access article under the CC BY-NC-ND license (<http://creativecommons.org/licenses/by-nc-nd/4.0/>).
2352-345X
<https://doi.org/10.1016/j.jcmgh.2018.01.013>

Received November 1, 2017. Accepted January 12, 2018.

Acknowledgments

The authors thank Nicholas O. Markham for editing the manuscript. The authors also thank Dr Vogelstein for the kind gift of parental DLD-1 and DLD-1 GLUT-1 KO cell lines.

Author contributions

Dennis K. Jeppesen, Qin Zhang, Michelle Demory Beckler, and Jeffrey L. Franklin designed and performed experiments, analyzed data, and wrote the paper; James N. Higginbotham designed and performed experiments; Emily J. Poulin, Alex J. Walsh, Eliot T. McKinley, Matthew R. Hight, Michael L. Schulte, Kimberly R. Watt, Melissa M. Wolf, and Gabriela Andrejeva performed experiments; Melissa C. Skala, H. Charles Manning, and Jeffrey C. Rathmell supervised the experimental design and analysis; G. Daniel Ayers performed statistical analyses; and Robert J. Coffey designed experiments, analyzed data, wrote the paper, and supervised the work.

Conflicts of interest

The authors disclose no conflicts.

Funding

Supported by National Cancer Institute grants R01 CA163563, U19 CA179514, R35 CA197570, and GI Special Programs of Research Excellence P50 CA 095103 (R.J.C.), NCI HCM R25 CA092043 (M.D.B.), and NIDDK DDRc pilot grant P30 DK058404 (J.L.F.). The Vanderbilt University Flow Cytometry Shared Resource and Center for Small Animal Imaging and the Radiochemistry Core Service are supported by the Vanderbilt Ingram Cancer Center (P30 CA68485) and the Vanderbilt Digestive Disease Research Center (P30 DK058404). The Radiochemistry Core Service also is supported by National Institutes of Health Shared Instrumentation grants S10 OD023543 and OD019963 (H.C.M.).

Supplementary Materials and Methods

Cell Culture and Reagents

DLD-1, DKs-8, DKO-1,¹ and DLD-1 GLUT-1 knockout cells were cultured as described previously.^{2,3} Propidium iodide was purchased from Invitrogen/Molecular Probes (Carlsbad, CA) and Hoechst was purchased from Sigma (St. Louis, MO).

Exosome Isolation and Characterization

Exosomes were isolated from conditioned medium of DKs-8, DKO-1, DLD-1, and DLD-1 GLUT-1 KO cells as previously described.² The diameter of exosomes (mean diameter, 50 nm) was obtained by nanoparticle tracking analysis (NanoSight, Wiltshire, United Kingdom; N = 4) as previously described.⁴ Electron microscopic imaging of exosomes was performed as previously described.⁴ Exosome pellets from DKO-1 cells were applied to the bottom of a discontinuous 5%–45% iodixanol (OptiPrep, Sigma-Aldrich) gradient and subjected to ultracentrifugation at $120,000 \times g$ for 16 hours at 4°C using a TH-641 swinging bucket rotor (*k* factor of 114; Thermo Scientific [Waltham, MA]). Fractions (1 mL) were collected from the top of the gradient. Each fraction was diluted in phosphate-buffered saline and subjected to ultracentrifugation at $120,000 \times g$ for 4 hours at 4°C using a SureSpin 630 (*k* factor of 219; Thermo Scientific) swinging bucket rotor.

Positron Emission Tomography Agent Synthesis

¹⁸F-Fluorodeoxyglucose was obtained commercially from PETNET (Siemens Healthcare Diagnostics, Inc, Tarrytown, NY) with an average radiochemical purity of 98.5% and specific activity of greater than 1000 Ci/mmol. ¹⁸F-FSPG was prepared as previously described.⁵

¹⁸F-Fluorodeoxyglucose Incorporation

A total of 50 μ Ci of ¹⁸F-fluorodeoxyglucose was added to 50 μ L of DKs-8, DKO-1 DLD-1, or DLD-1

GLUT-1 KO cell-derived exosomes (1 mg/mL) in phosphate-buffered saline–HEPES, pH 7.2, and these samples were incubated at 37°C for 1 hour. Ethylenimine (0.05%; Sigma) then was added and the solution was placed on an Isolete Phase Separator (Biotage, Charlotte, NC) fitted with a GF/B filter (Brandel, Inc, Gaithersburg, MD). Filters were washed, removed, and radioactivity was measured. Analysis was performed on at least 3 independent preparations of exosomes.

Immunoblot Analysis

Immunoblotting of cell lysates and exosomes was performed as previously described.^{3,4} Primary antibodies were epidermal growth factor receptor (1:1000; Millipore, Burlington, MA), syntenin-1 (1:5000; Abcam, Cambridge, MA), CD81 (1:1000; R&D Systems, Minneapolis, MN), GLUT-1 (1:1000; mouse; Abcam), GLUT-3 (1:1000; Abcam), and Alix (1:10,000; Cell Signaling, Danvers, MA). Secondary antibodies were rabbit IgG, horseradish peroxidase–linked antibody (1:1000; Sigma); mouse IgG, horseradish peroxidase–linked (1:5000; Jackson ImmunoResearch, West Grove, PA); and IR-800 antibody (1:15,000; LI-COR, Lincoln, NE). Immunoblots were imaged by fluorescence detection using an Odyssey Fc Imaging System (LI-COR).

Measurement of Cellular Glucose Consumption

Before plating, 5×10^5 DKs-8 cells were incubated with 50 μ g exosomes or mock treated for 1 hour at 37°C. Cells were plated in 48-well dishes at 24,000 cells per well (in triplicate). Dulbecco's modified Eagle medium containing 5 mmol/L glucose (Sigma) and 3% fetal calf serum was added to each well. At the indicated times, medium was removed and stored at -80°C, and cell number was counted by measuring the fluorescent intensity of SYBR green (Invitrogen) staining. Glucose concentration in the medium was measured (normalized to cells per well, N = 3 in triplicate) using the Glucose Colorimetric Assay Kit (Cayman Chemical, Ann Arbor, MI), according to the manufacturer's directions.

Analysis of Cell-Cycle Progression

Before plating, 1.0×10^6 DKs-8 cells were incubated with 100 μ g exosomes or mock treated for 1 hour at 37°C, plated in 10-cm tissue culture dishes and Dulbecco's modified Eagle medium containing 5 mmol/L glucose, and 3% fetal calf serum was added and incubated for the indicated times. A total of 2 μ g/mL of Hoechst 33342 (Sigma) was added to each plate 1 hour before harvest. Fifty thousand cells were washed and resuspended in 500 μ L of phosphate-buffered saline supplemented with 3% fetal calf serum and the cell cycle was analyzed by flow cytometry. Samples were analyzed on a BD LSR II (Franklin Lakes, NJ) equipped with a solid-state UV laser. Doublet discrimination was used with appropriate pulse geometries⁶ (n = 3 in triplicate).

Isolation and Culturing of Mouse Colonic Cells

This procedure was performed as previously described.^{7,8}

Optical Metabolic Imaging

After trypsinization and washing, DKs-8 or mouse colonic epithelial cells were centrifuged and resuspended at 1×10^6 cells/mL in high-glucose Dulbecco's modified Eagle medium containing 3% fetal calf serum. Medium was supplemented with 100 μ g/mL DKs-8 or DKO-1 cell-derived exosomes or 100 μ L phosphate-buffered saline. Cells were incubated at 37°C for 60 minutes. Twenty thousand cells per well were plated in 24-well dishes and incubated for 48 hours at 37°C, and then optical metabolic imaging was performed. For colonoid experiments, cells were cultured in Matrigel (Corning, Tewksbury, MA) using minigut medium and then placed in 24-well agar-coated dishes. A total of 100 μ g of DKs-8 or DKO-1 exosomes or 100- μ L phosphate-buffered saline were added to the 400 μ L of minigut medium in each well and orbitally rocked at 37°C for 1 hour followed by a 48- or 96-hour incubation at 37°C and then imaged.

Multiphoton optical metabolic imaging microscopy of NADH and FAD was performed on a custom-built, multiphoton fluorescence microscope (Bruker, Bremen, Germany), as previously described.^{9–11} Individual cells within the image were segmented using a customized routine in CellProfiler (Carpenter Lab at the Broad Institute of Harvard and MIT, Cambridge, MA)¹² and the mean redox ratio for each cell was computed as the ratio of NADH fluorescence intensity divided by FAD fluorescence intensity.

In Vivo Imaging

All procedures were approved by and performed in accordance with Vanderbilt University Animal Care and Use Committee guidelines. *Apc*^{Min/+} or WT (non-tumor-bearing) mice were screened for colonic tumors by colonoscopy. Before imaging, mice were injected for 4 consecutive days with 300 μ g of DKs-8 or DKO-1 exosomes in 500 μ L of phosphate-buffered saline. Mock-treated mice were injected with 500 μ L of phosphate-buffered saline. For ¹⁸F-FSPG positron emission tomography imaging, mice were imaged with microPET Focus 220 (Siemens Preclinical Solutions, Knoxville, TN) and NanoSPECT/CT (Bioscan, Washington, DC) 2 hours after the final exosome or mock injection as previously described.^{13,14} Regions-of-interest determination was guided by anatomic magnetic resonance images (Varian, Inc, Palo Alto, CA). Similar-sized regions-of-interest were drawn around the tumors and hind limb muscles. The ¹⁸FSPG signal was expressed as the tumor-to-muscle uptake ratio. Comparisons between groups were performed using a 1-way analysis of variance followed by a Tukey test. For magnetic resonance images, multislice scout images were collected in all 3 imaging planes (axial, sagittal, and coronal) using a gradient echo sequence with a repetition time of 75 ms, echo time of 5 ms, slice thickness of 2 mm, flip angle of 35°, and an average of 4 acquisitions. Additional parameters included field of view of 50 mm \times 50

mm and data matrix of 128 \times 128 pixels.

Tissue Preparation

Tissue were processed as previously described,¹⁵ except after positron emission tomography imaging when representative colonic tumors were dissected, they were then placed in Dulbecco's modified Eagle medium containing 10% fetal calf serum, and subjected to optical metabolic imaging.

Proton Magnetic Resonance (¹H-MRS) of Cell Culture Media

Before plating, 5 million DLD-1 GLUT-1 KO cells were incubated with 500 μ g exosomes isolated from parental DLD-1 cells or DLD-1 GLUT-1 KO cells, or mock treated for 1 hour with rotation at 37°C. Cells were plated in 10-cm dishes with 5 million cells per dish (in triplicate) with Dulbecco's modified Eagle medium containing 10% fetal calf serum depleted of bovine exosomes as previously described.¹⁶ After 43 hours, fresh cell culture medium and cell-conditioned medium were collected for metabolite measurements. A total of 50 μ L D₂O (Sigma-Aldrich) and 50 μ L of 0.75% sodium 3-trimethylsilyl-2,2,3,3-tetradeuteropropionate in D₂O (Sigma-Aldrich) were added to 500 μ L media in 5-mm NMR tubes (Wilmad-LabGlass, Kingsport, TN) for chemical shift calibration and quantification. ¹H-MRS spectra were acquired on an Avance III 600 MHz spectrometer equipped with a Triple Resonance CryoProbe (TCI) (Bruker) at 298 K with 7500-Hz spectral width, 32,768 time domain points, 32 scans, and a relaxation delay of 2.7 seconds. The water resonance was suppressed by a gated irradiation centered on the water frequency. The spectra were phased, manually baseline corrected, and referenced to sodium 3-trimethylsilyl-2,2,3,3-tetradeuteropropionate using the Bruker TopSpin-3.5 software package. Spectral assignments were based on literature values.¹⁷

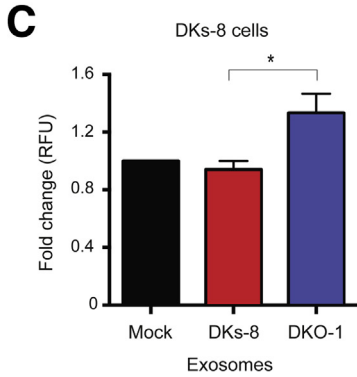
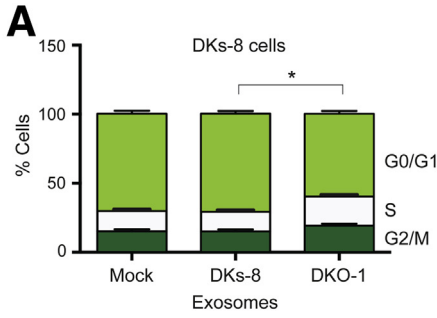
Statistical Methods

All analyses were conducted within the framework of mixed models

analysis of variance. Variation between experiments conducted on separate days was modeled as a random effect. Data transformations were evaluated to meet normality assumptions. Repeated measures in sampling (eg, multiple fields analyzed within mice from the *in vivo* study) were modeled using a compound symmetry covariance structure. Goodness-of-fit was evaluated via analysis of model residuals. Comparisons between groups were performed as described earlier. Statistical analysis was conducted using GraphPad Prism version 6 for Mac OS X (Cupertino, CA) (GraphPad Software, Inc, San Diego, CA).

References

1. Shirasawa S, et al. *Science* 1993; 260:85–88.
2. Demory Beckler M, et al. *Mol Cell Proteomics* 2013;12:343–355.
3. Higginbotham JN, et al. *Curr Biol* 2011;21:779–786.
4. Higginbotham JN, et al. *J Extracell Vesicles* 2016;5:29254.
5. Kavanaugh G, et al. *Mol Imaging Biol* 2016;18:924–934.
6. Darzynkiewicz Z, et al. *Curr Protoc Cell Biol* 2001;Chapter 8:8.4.
7. Sato T, et al. *Nature* 2009; 459:262–265.
8. Whitehead RH, et al. *Am J Physiol Gastrointest Liver Physiol* 2009; 296:G455–G460.
9. Walsh A, et al. *Biomed Opt Express* 2012;3:75–85.
10. Walsh AJ, et al. *Cancer Res* 2013; 73:6164–6174.
11. Walsh AJ, et al. *J Biomed Opt* 2012;17:116015.
12. Walsh AJ, Skala MC. *Proc. SPIE Multiphoton Microscopy in the Biomedical Sciences XIV* 2014; 8948:89481M.
13. Hassanein M, et al. *Mol Imaging Biol* 2016;18:18–23.
14. McKinley ET, et al. *PLoS One* 2014; 9:e108193.
15. Powell AE, et al. *Cell* 2012; 149:146–158.
16. Jeppesen DK, et al. *J Extracell Vesicles* 2014;3:25011.
17. Govindaraju V, et al. *NMR Biomed* 2000;13:129–153.



B 24 hours

Exosomes	G0/G1	S	G2/M
-	56% +/- 2.08	26.6% +/- 1.18	18% +/- 1.5
DKs-8	55.5% +/- 2.08	21.2% +/- 1.18	17.9% +/- 1.5
DKO-1	41.1% +/- 2.08*	34.7% +/- 1.18*	22% +/- 1.5*

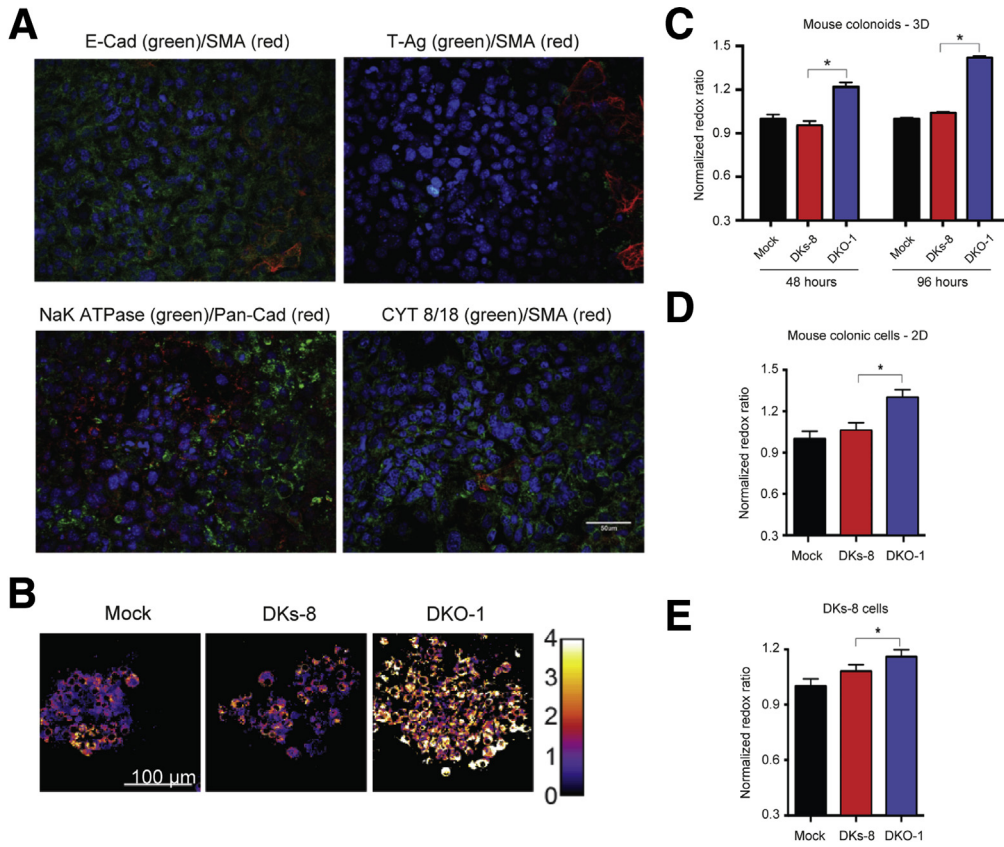
48 hours

Exosomes	G0/G1	S	G2/M
-	70.4% +/- 1.89	14.7% +/- 1.02	15.2% +/- 1.45
DKs-8	71% +/- 1.89	14.3% +/- 1.02	15.1% +/- 1.45
DKO-1	59.8% +/- 1.89*	21.2% +/- 1.02*	19.2% +/- 1.45*

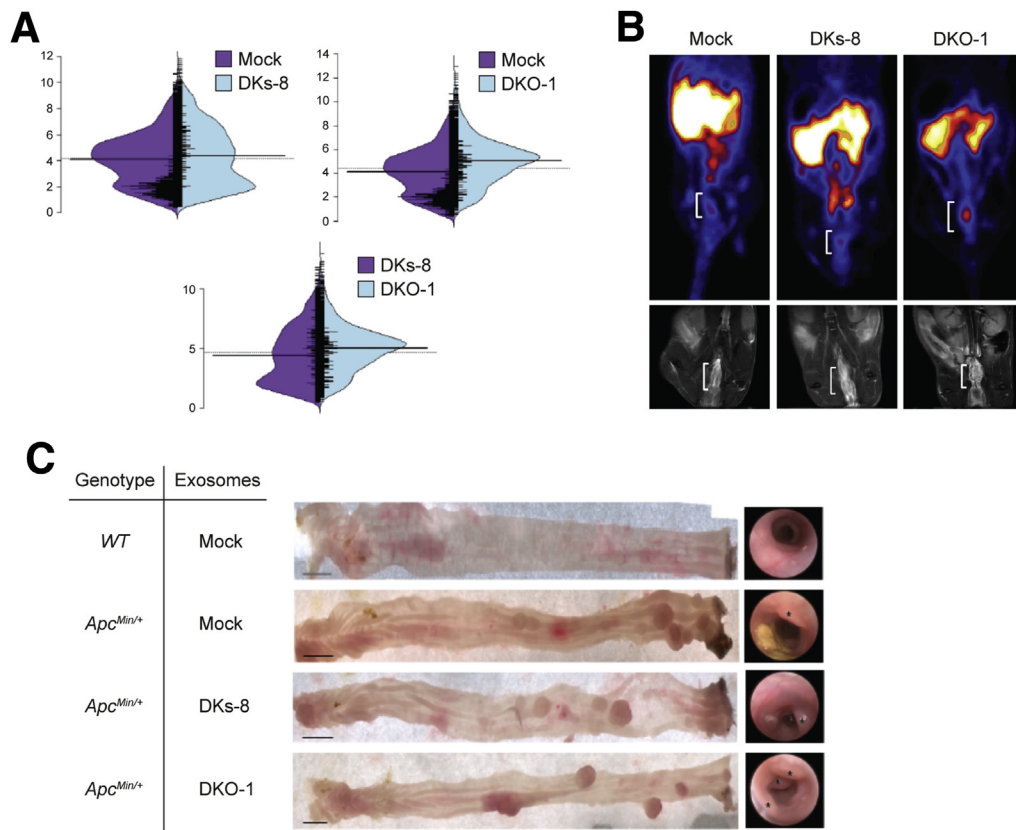
72 hours

Exosomes	G0/G1	S	G2/M
-	74% +/- 2.08	12.8% +/- 1.18	12.4% +/- 1.5
DKs-8	75.8% +/- 2.08	15.9% +/- 1.18	12.3% +/- 1.5
DKO-1	67.6% +/- 2.08*	12.3% +/- 1.18*	26.6% +/- 1.5*

Supplementary Figure 1. Mutant KRAS exosomes enhance cell-cycle progression and proliferation of DKs-8 cells cultured in low-glucose medium. DKs-8 cells were incubated with DKs-8 or DKO-1 exosomes or mock-treated (A) for 48 hours or (B) for times shown. Cell-cycle state was assayed by Hoechst staining followed by flow cytometric analysis (n = 3 in triplicate). (C) Growth of exosome-treated DKs-8 cells after 120 hours as determined by relative fluorescence intensity (RFU) of stained nuclei. (A and C) *P < .05 for comparison indicated. (B) *P < .05 for pairwise comparisons between DKO-1 exosomes vs DKs-8 exosomes or mock treatment.



Supplementary Figure 2. Characterization of exosome effects in vitro. (A) Normal mouse colonoid cultures were characterized by antibody staining as indicated. Most epithelial cells express non-cell-surface E-cadherin (E-Cad; green); smooth muscle actin (SMA; red) marks pericryptal fibroblasts. T-antigen (green) indicates the presence of young adult mouse colon (YAMC) cells. Na/K adenosine triphosphatase (ATPase) (green) marks epithelial cells separate from Pan-Cadherin-expressing cells. Most epithelial cells express cytokeratin (CYT) 8/18 (green). (B) Representative images for panel C. Redox ratios for (C) normal mouse colonoids cultured in Matrigel, (D) normal mouse colonic cells cultured on plastic, and (E) DKs-8 cells exposed for 48 hours to the treatments indicated. Data are mean normalized redox ratio \pm SEM. * $P < .05$.



Supplementary Figure 3. Metabolic imaging in vivo. WT or *Apc^{Min/+}* mice were injected with DKs-8 or DKO-1 exosomes or mock-treated. (A) Colonic tumors were removed and the normalized redox ratio was calculated. Y-axis plots redox ratios of individual cells showing distribution of ratios for pair-wise comparisons. Mutant KRAS DKO-1 exosomes show a shift toward higher redox ratios. (B) ^{18}F -FSPG uptake was monitored by positron emission tomography imaging; representative positron emission tomography images are shown with brackets highlighting colonic regions of interest with corresponding magnetic resonance image in bottom panel. (C) Whole-mount and colonoscopic images from mice in each treatment group. *Distal colonic tumors.

Supplementary Figure 4. Morphologic and biochemical analysis of exosomes. (A) DKO-1 exosomes show characteristic appearance by transmission electron microscopy (Materials and Methods). (B) DKs-8 and DKO-1 exosomes have a similar mean particle diameter. Four independent preparations of DKs-8 and DKO-1 exosomes were subjected to nanoparticle tracking analysis (Materials and Methods). Data are plotted as average diameter \pm SD. (C) Immunoblot analysis of DKO-1 cell-derived exosomes fractionated by iodixanol density gradient centrifugation. (D) Immunoblot analysis of DLD-1 parental and GLUT-1 KO cells and exosomes.

